The topological reconstruction of forced oscillators

Hernán G. Solari[1] and Mario A. Natiello[2] *

[1] *Departamento de Física, Facultad de Ciencias Exactas y Naturales, Universidad de Buenos Aires, Ciudad Universitaria, Pab I 1428 Buenos Aires, Argentina.*

[2] *Center for Mathematical Sciences, Lund University, Box 118, 221 00 LUND, Sweden.*

* *Corresponding author: email* `Mario.Natiello@math.lth.se`*, fax: +46 46 222 4010.*

February 23, 2009

Abstract

Periodically forced oscillators are among the simplest dynamical systems capable to display chaos. They can be described by the variables position and velocity, together with the phase of the force. Their phase-space corresponds therefore to $R^2 \times S^1$. The organization of the periodic orbits can be displayed with braids having only positive crossings. Topological characterization of dynamical systems actually began to be explored in physics on this family of problems.

In this work we show that, in general, it is not possible to produce a 3-dimensional imbedding of the solutions of a forced oscillator in terms of differential imbeddings based on sampling the position only. However, it may be possible to uncover a description of the phase variable from the sampled time-series, thus producing a faithful representation of the data. We proceed to formulate new tests in order to check whether proposed imbeddings can be accepted as such.

We illustrate the manuscript throughout with an example corresponding to a model of Benárd-Marangoni convection.

1 Introduction

Given that two-dimensional ordinary differential equations (ODE) cannot display chaos, the next-simplest choice in the search for chaos and its consequences are 3-dimensional systems. In particular, periodically forced nonlinear oscillators of one degree of freedom can produce flows and Poincaré (stroboscopic) maps displaying chaos. Some of these systems have gained a particular fame such as the Duffing oscillator [1] and the van der Pol oscillator [2] (see a review on both oscillators in [3]). Furthermore, these oscillators can be constructed as

physical devices (often electronic or mechanical). Periodically forced oscillators or equivalent devices can also be constructed modulating the pumping in class B lasers [4].

The restrictions determined by the 3-dimensional phase-space impose a rigid structure to the periodic orbits of the oscillator for any given parameter value. This structure, a 3-dimensional analogue of Sarkovskii's order [5, 6], encapsulates in the form of braids much of the information of the chaotic sets of forced oscillators [7, 8, 9, 10, 11, 12, 13, 14, 15].

The orbit structure of periodically forced oscillators began to be studied in physics during the 80's [16, 17]. Methods to make contact with experiments followed [18, 19]. These methods rested upon time-delay and differential imbeddings. While Takens' imbedding theorem [20, 21] does not directly apply to periodically forced systems, an extension of Takens theorem, that applies to forced oscillators, exists [22]. These theorems suggest the possibility of reconstructing the attractors of forced oscillators in 6 [23] or 7 [24] dimensions, which are in any case too many, considering that the topological methods exploiting the braid structure yield nontrivial information only in (or up to) three dimensions.

It has being argued that although the theorems do not suggest a 3-dimensional imbedding reconstruction, they do not forbid it either. Finding a good 3-dimensional imbedding and checking imbedding qualities became a craft or art which rested heavily on the False Neighbours method [25]. Up to the present days, derivative- or delay-imbeddings inspired in Takens[20] are often used to attempt a reconstruction of the dynamics of forced oscillators using 3 dimensions [26, 27, 28, 29, 30] or more[31], at different levels of detail and accuracy. One of the results of this manuscript is that 3-dimensional imbeddings of this kind cannot provide a **complete** dynamical reconstruction of phase space except when a specific additional condition is met.

Three new pieces of information contributed in the 90's to a better understanding of the situation. In the first place, a work by McRobie [32] showed with a simple theorem that in the $R^2 \times S^1$ presentation of the braids associated to periodically forced oscillators in the natural coordinate system (x, v, ϕ) (i.e., position, velocity, phase), only positive crossings can be present. The second contribution was produced in a series of works by Mindlin and collaborators. A model of a periodically forced Takens-Bogdanov bifurcation was introduced in relation to the description of a low aspect-ratio Benárd-Marangoni experiment [33]. The reconstruction method shows an important sensitivity to the number of spatial modes included in the description of the pattern [34] and the braids produced in the reconstruction based upon the "position" coordinate displayed positive as well as negative crossings.

The third piece of information was presented in [35], where it was shown that different attempts to imbed the data produced topologically inequivalent reconstructed orbits, in terms of their braid content and properties. This problem, known as the "topological inequivalent imbeddings", was later addressed in [36, 37], proposing a resolution of the apparent contradiction.

In this work we will address the specific problem of producing a three-

dimensional imbedding out of the output recorded from a single variable of a periodically forced oscillator. For such a system we will prove a Lemma indicating that although it might be possible to imbed a periodic orbit or perhaps an attractor, it is not possible to extend the imbedding to the full phase-space and hence, no conclusions can be drawn from the imbedded data regarding regions not visited by the data.

The present research leads to the re-evaluation, in the light of the Lemma, of the false neighbours method [25]. We will then show that checking the differential structure of the imbedded flow produces useful acceptance/rejection criteria beyond "false neighbours". Finally, the same ideas involved in the Lemma are used to produce a simple test that detects the clock of a forced system, and allows for the reconstruction of the original phase space $R^2 \times S^1$, beyond the realm of delay imbeddings.

We start by freshening up the desired goals of imbeddings used within applied dynamical systems theory (Section 2). Next, we review the basics of periodically forced oscillators with a specific example (Section 3). We then prove a simple result showing that in general terms, in the case of periodically forced oscillators it is not possible to produce a 3-dimensional differential imbedding (and related geometrical objects) based in one measured coordinate only (Section 4). We offer new and more sensible numerical criteria to probe the quality of a proposed imbedding (Section 5). Further, we describe how the phase-space reconstruction of periodically forced oscillators can be implemented (Section 6). Further, we address the issue of "topologically inequivalent imbeddings" in Section 7. Finally, Section 8 presents the concluding remarks.

2 Revisiting the imbedding paradigm

In Appendix I we review some basic material about the imbedding theorems. An important question in applications is: "What do we want imbeddings for?" In practice, we start with a time-series obtained by some experiment, i.e., a discrete set of values of some function $y(x(t))$, just because *this is what it is possible to produce experimentally.* But what we really would like to have is a description of the original phase-space where the system was evolving. Ideally, if Takens' idea works, letting y be the "projection onto the first coordinate", we record one coordinate, and after some manipulation we generate a dynamic evolution on an Euclidean space of not very large dimension. In experimental science, hence, we would like to have much more than just an imbedding. We would like to have a dynamical description that works even in the "empty" space where we do not have recorded data. The bad thing is that perhaps we have much less. The words "almost any", "generically" and "residual set", appearing in different statements of Takens' imbedding theorems indicate that just our particular problem and choice of measuring function, may *not* be an imbedding. Hence, imbedding candidates have to be tested a posteriori. The procedure starts by proposing an imbedding candidate, generating higher-dimensional dynamical data and finally checking that the map from the original system to the generated data has a

fair chance of being 1-to-1 and immersive. This has to be done within some tolerance level, since experimental data has finite precision and sufficiently large time-series will in general fail to map 1-to-1 onto the target space.

Another side-question is the fact that the usual imbedding practice uses a discrete data record, i.e., data taken at discrete time-intervals. Since Takens' imbeddings are based on a continuous-time measuring function $y(x(t))$, the discrete sampling has to be subject to the standard controls in experimental science, i.e., the sampling interval has to be sufficiently short so that a continuous function interpolated from data has a fair chance to describe the original complexity in the system. For example there are laser experiments where the relevant dynamics has a low-frequency variation combined with a high-frequency effect. To naively set the sampling frequency according to the low-frequency part, renders the rest of the dynamics essentially invisible [38, 39].

It remains true that experimental data series are finite in the number of samples, as well as finite in their precision. The data available is then a "zero-dimensional" data set (and hence lying *outside* the range of validity of Whitney's and Takens' imbedding theorems).

From the "zero dimensional" recorded data set, a one-dimensional manifold (a portion of an orbit) is conjectured in the first place (thus coming back to the validity range of Whitney and Takens through active intervention of the scientist, in the form of an interpolation recipe). Next, a strange attractor is conjectured and finally a smooth manifold where the attractor lies is conjectured.

It is useful to have in mind that if $f : M \to N$ is an imbedding of the manifold M, then there is an inverse map from $f(M)$ to N by the definition of imbeddings. Hence, in the case of forced oscillators where $M = R^2 \times S^1$ if we find two different imbeddings, f and g, of the full phase space M, provided we have chosen conjugated Poincaré sections on each one, then f and g conjugate the phase space with the orbits in them and their periodic structure into $f(M)$ and $g(M)$, hence, the braid type[40] is preserved. In this perspective, restricting the reconstructed phase space to the interior of a well sampled bounding torus, as discussed in [36, 37], effectively preserves the available topological information.

3 Takens-Bogdanov forced system

We start with the basic definition. A *periodically forced oscillator* responds to the following ordinary differential equation

$$\begin{aligned} \dot{x} &= v \\ \dot{v} &= f(x, v, t) = f(x, v, t + T) \end{aligned} \tag{1}$$

with T the minimal period of the function $f(x, v, t)$. Given that f is Lipschitz, there is one solution and only one passing through the point (x, v, ϕ), where the third coordinate is a phase in $[0, 2\pi/T]$. The coordinate ϕ arises naturally by recasting the above time-dependent dynamical system as an autonomous system. The resulting phase-space is the abstract space $R^2 \times S^1$.

Experimental results corresponding to a Benárd-Marangoni flow in a square container were first put into correspondence with a Takens-Bogdanov bifurcation [41], thus deriving an ODE for the experiment that actually represents an oscillator in one of the (equivalent) normal forms [42]. When the experiment was repeated adding a periodic forcing it was natural to model the problem with a periodically forced oscillator of the form [33]:

$$\begin{aligned} \dot{x} &= v \\ \dot{v} &= R(t)(\mu x + \nu v) + x^2(v - x) \\ R(t) &= 1 + \epsilon \cos(\omega t). \end{aligned} \tag{2}$$

Also this equation can be recasted as an autonomous system (as will be done below) by replacing t with the phase ϕ in R and adding the additional equation $\dot{\phi} = 1$.

We will use some of the chaotic attractors of (2) in the examples of the coming sections. Because of this reason we introduce them here. For $\mu = 1.0434$, $\nu = -1$, $\omega = 0.399$ and $\epsilon = 0.45$ the system of eq.(2) shows two separated attractors related by a rotation $(x, v, t) \to (-x, -v, t)$. Each attractor intersects the control section $\{v = 0,\ \dot{v} > 0\}$ in three non-intersecting regions, each one including points close to a periodic orbit of stroboscopic-period one. However, if the system is further explored, say for $\epsilon = 0.452$ while keeping the other parameters as above, the period-1 orbit at $\epsilon = 0.45$ can be continued without problems onto its modified version at $\epsilon = 0.452$ with the additional observation that the attractor no longer intersects the control section in three non-intersecting sets. Rather, the three "islands" have merged and other regions of the attractor are visited (see Figure 1).

4 A lemma on the imbedding of periodically forced oscillators

In view of the situation depicted in Section 2, the theorems by Takens [20] and Stark [22] based upon the ideas of Whitney [24], represent indications of whether we can expect to be lucky or not with our conjectured system. The reconstruction of 3-dimensional systems with 3-dimensional imbeddings requires additional elements and tests applicable to data.

In [43, 44] the authors explore changes of coordinates transforming (x, y, z) into $(X, Y, Z) = (x, \dot{x}, \ddot{x})$ for different 3-dimensional autonomous systems known to have chaotic attractors among their solutions (Lorenz, Rössler, and others). The proposed differential 3d-imbeddings present two kinds of difficulties: (a) some of the transformations are many-to-one (projections), while (b) other transformations present singularities on sub-manifolds of dimension smaller than 3. Both difficulties may appear simultaneously.

These difficulties might not be completely invalidating. Concerning (a), the sampled data may visit just one branch of the (multivalued) inverse map and then, the transformation restricted to the actual data may still be invertible.

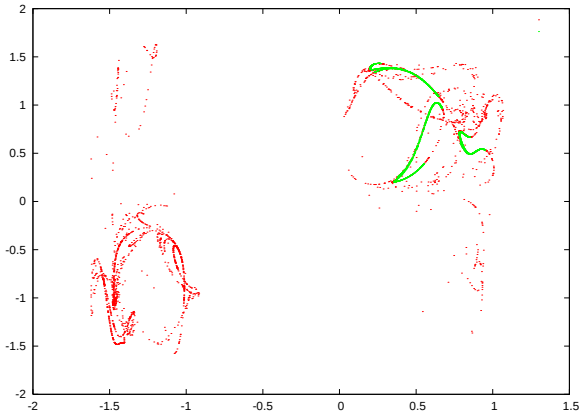

Figure 1: Intersection of reconstructed data of eq. (2) with the control surface $\{v = 0,\ \dot{v} > 0\}$ for delay ($\tau = 205$). Green color, solid line, $\epsilon = 0.45$: three islands can be seen (on the upper right corner). Red color, dotted, $\epsilon = 0.452$: the islands have merged and other regions of the attractor are visited. The variables (x, t) intersecting the control section are plotted as $(e^x \cos \omega t, e^x \sin \omega t)$.

In the same form concerning singularities in (b), the attractors and conjectured manifolds need not intersect the singular set (once again, tests should be devised to assert the reasonability of the theoretical reconstruction).

The corresponding analysis for forced oscillators is as follows.

Lemma 1 *Differential imbeddings for forced oscillators. Let*

$$\Phi_t(x_0, v_0, \phi_0) = (x(t), v(t), \phi(t))$$

be the time-evolution given by eq.(1) (recasted as an autonomous system) of an arbitrary initial condition $(x(0), v(0), \phi(0)) = (x_0, v_0, \phi_0)$. *Let the map*

$$\mathcal{B}F : (x, v, \phi) \to (x, \dot{x}, g(x, v, \phi))$$

be the proposed imbedding for the solutions of eq.(1), where $g(x, v, \phi))$ *is a real function, differentiable in its three variables, and* 2π*-periodic in* ϕ.

Then, $\mathcal{B}F$ *is a projection that does not commute with the flow (i.e., for a large set of initial conditions, two different initial conditions with the same projection yield different projected dynamics).* □

Before sketching the proof, let us explore the implications of the result. Examples of such functions g may be the rhs of $\dot{v}$ in eq.(2) or the first component of $\Phi_{-\tau}(x_0, v_0, \phi_0)$ for fixed delay τ (i.e., differential or delay imbeddings for the third coordinate). The lemma implies that a transformation such as $\mathcal{B}F$ requires additional, *ad hoc* and fine-tuned analysis before being accepted as an imbedding, and that **it will or will not be a imbedding depending of the**

particularities of the solution to be studied. Thus, e.g., the bona-fide procedure applied to the attractor of eq.(2) for $\epsilon = 0.45$, even if it would have worked in that case (generating an acceptable imbedding), may or may not yield an imbedding for $\epsilon = 0.452$. These facts further stress the difficulties emerging from non-sampled areas of the phase-space as well as the need of finding support in the data to asses the validity of bona-fide procedures.

PROOF It is evident from the first line in eq.(1) that for our purposes $\dot{x}$ is identical to v throughout. Since $g(x, v, \phi)$ is real, continuous and periodic, for each fixed pair (x, v), the function g can be seen as a (differentiable) function of $\phi \in [0, 2\pi]$ and as such it attains its maximum and minimum values in the interval. For any value $\bar{g}$ lying between these extreme values, $g(x, v, \phi) = \bar{g}$ has at least two solutions. Hence, with the possible exception of both extreme values, for every point $(x, \dot{x}, \bar{g})$ in the proposed imbedding there are at least two possible pre-images (x, v, ϕ_1) and (x, v, ϕ_2) in the original phase-space. Hence, $\mathcal{B}F$ is a projection (from phase-space to "imbedding space").

Consider now two different points in $R^2 \times S^1$ corresponding to the same point in the projection, say $X = (x, v, \phi_1)$ and $Y = (x, v, \phi_2)$ along with their respective time-evolution given by the flow associated to eq.(1), $X(t)$ and $Y(t)$, where $X(0) = X$ and $Y(0) = Y$. The third coordinate, ϕ, evolves in each case as $\phi_i(t) = \phi_i + 2\pi \frac{t}{T} \bmod 2\pi$, $i = 1, 2$. Assume further that $\phi_2 > \phi_1$ and that there is no other solution of $g(x, v, \phi) = \bar{g}$ between ϕ_2 and ϕ_1. Let finally $0 < \theta = \phi_2 - \phi_1 < 2\pi$.

Since $f(X(0)) = f(Y(0))$, the initial condition of both dynamical orbits lies on the (implicitly defined) two-dimensional sub-manifold of phase-space,

$$\mathcal{PR} = \{f(x, v, \phi) - f(x, v, \phi + \theta) = 0\}.$$

The projection commutes with the flow only along orbits lying completely within this manifold for $t \neq 0$. Geometrically, the time derivative of $\mathcal{PR}$ along the flow has to be zero (the vector field has zero scalar product with the normal vector of the manifold, or, intuitively, the points on the manifold follow their dynamics without leaving the manifold), i.e.,

$$\nabla(f(x, v, \phi) - f(x, v, \phi + \theta)) \cdot (v, f(x, v, \phi), 1) = 0.$$

This condition also defines a two-dimensional sub-manifold of phase-space. On the intersection of both manifolds lie the orbits along which the projection $\mathcal{BF}$commutes with the dynamics. Outside this (small[1]) set of orbits, the projection does not commute with the flow, and the projected dynamics for a given pre-image will differ from the projected dynamics of the other pre-image(s). ■

A simple corollary of the Lemma is that no delay imbedding of a forced oscillator can be extended to the full phase space.

[1]The intersection of two 2-d manifolds in 3-space can at most be a 2d-manifold itself (if, e.g., one manifold is a subset of the other). In general it will be a finite set of 1-d manifolds (transverse intersection) and in exceptional cases it could be a discrete or even empty set.

Let us illustrate the proof with eq.(2) and a differential bona-fide procedure. Let $\mathcal{B}F(x, v, \phi) = (x, \dot{x}, \ddot{x})$. From eq.(2) we obtain

$$(\mu x + \nu \dot{x})\epsilon \cos(\phi) = \ddot{x} - x^2(\dot{x} - x) - (\mu x + \nu \dot{x}).$$

For each projected point away from $\phi = 0$ or $\phi = \pi$ we have two different pre-images, which by the properties of the cosine function will yield different dynamics, unless we move along the manifold $\mathcal{PR} = \{(x, v, \phi) : \mu x + \nu \dot{x} = 0, \phi \in [0, 2\pi]\}$. Yet $\mathcal{PR}$ as a whole is not invariant with respect to the flow, since its time-derivative following the flow is:

$$\mu \dot{x} + \nu(R(t)(\mu x + \nu \dot{x}) + x^2(\dot{x} - x)) = -x(\mu^2 + x^2(\nu + \mu))/\nu.$$

Hence, the only orbit lying completely on the two dimensional manifold (for general values of ν, μ) is $(0, 0, \phi)$, certainly a particular solution of the problem. Outside this solution, the bona-fide procedure is a projection that does not commute with the flow.

5 Testing proposed imbeddings techniques beyond false neighbours

The result offered by Lemma 1, makes clear that only in exceptional cases[2] the standard procedures based in the position coordinate might give an acceptable 3-dimensional reconstruction of periodically forced oscillators (i.e., only if the recorded data systematically avoids all but one branch of the inverse map). However, to develop and improve tests of the quality of proposed imbeddings is still proper, since there has been some confusion around the concepts. Also, the (new and old) tests presented in this manuscript are relevant in a wider perspective, since they do not depend on the choice of imbedding procedures and will be useful when alternative methods are considered.

Lemma 1 also suggests that the distinctive sign of an imbedding is to induce a flow in the imbedding space from the flow generating the data. We will use this property to produce a test complementary to the standard tests.

Basically, an imbedding is a 1-to-1 mapping with nonsingular derivative at each point. To "test" a proposed bona-fide procedure ($\mathcal{B}F$-*imbedding* in what follows, but recall that it is *not* an imbedding until we present satisfactory support in its favour) requires estimating both properties some way or the other. Additionally, since we often do not know the dynamical details of the system generating experimental data, some test to determine a reasonable "imbedding dimension" is necessary. The main ideas in terms of testing $\mathcal{B}F$-imbeddings has been since long ago detecting *false neighbours* [25].

The intuition behind the method is to establish if two portions of the data lying far enough in the time-order come too close to each other (e.g., closer

[2]Such exceptional cases did not occur in any of the computations performed for this manuscript.

than a certain threshold chosen by the scientist). This detection is a first step, requiring further analysis to assess its consequences.

If the $\mathcal{B}F$-imbedding was in fact a projection, adding an extra dimension may lift apparent intersections and remove false neighbours. We interpret this result as suggesting that the imbedding dimension was too low, and retry the procedure in higher dimensions. Eventually, an optimal imbedding dimension is obtained: the lowest possible with no more false neighbours than what we are prepared to tolerate

This is indeed the idea implemented in [35] and many other works of the time. In formulæ, consider an m-dimensional $\mathcal{B}F$-imbedding given by the points $x_{i,m} = (x_i^1, \ldots, x_i^m)$, then, $x_{i,m}$ is considered a false neighbour (at the ϵ level) of $x_{j,m}$ if $d(x_{i,m}, x_{j,m}) < \epsilon$ but $d(x_{i,m+1}, x_{j,m+1}) > \epsilon$. The process is cumulative, i.e., the first m components of $x_{i,m+1}$ coincide with $x_{i,m}$. Also, d is a suitable distance for each dimension, usually the Euclidean distance.

If the data does indeed have interesting topological information, some detected false neighbour candidates will persist even up to very large imbedding dimensions. In fact, the related method of *close returns* [45] used to determine if some portions of the data may lie close to an unstable periodic orbit of the original system, rests upon the fact that the data returns very close to itself after some time T_p (the period of the shadowed orbit), and moreover that this close return occurs not only for an isolated point in the data set but for a relatively large consecutive set of points. Periodic orbits of period p (in sampling-time units) are detected when $L \gg 1$ consecutive points are found, such that $d(x_{i,m}, x_{i+p,m}) < \epsilon$ for $i = 1, \cdots, L$. There is only a qualitative difference between a close return and a false neighbour: In the first, the near crossing of portions of data is almost tangent, and occurs for L consecutive points with the same p-interval and in many different dimensions. In the second, the near crossing is transverse, and ideally it occurs up to some dimension q but not for dimension $q + 1$. It is somewhat insatisfactory that the same test (close return of distantly sampled points) is used both to reject imbeddings and to accept periodic orbits. We introduce here two tests that still can detect unappropriate imbedding candidates, although without interference from the occurrence of periodic orbits.

If the $\mathcal{B}F$-imbedding was in fact a projection, we may further profit of this fact to improve the test. A possible scenario is that the experimental sampling visits two regions of phase-space lying far away from each other but having very similar projections. In such a case we have no imbedding and the proposed procedure should be rejected. However, this situation might be disguised as a close return. An orbit starting in region 1 and eventually shifting to region 2 could be seen after projection as a portion of data closing onto itself. When a close return in the data is found, it may be related either to a close return in the original phase space of the problem (*true* close return) or to a close return arising because of the projection (*false* close return). How to distinguish both situations? We consider here some alternatives.

Since the only accessible information is in the recorded data, we can ask whether the time-sequence of points in a $\mathcal{B}F$-imbedding represents a flow or

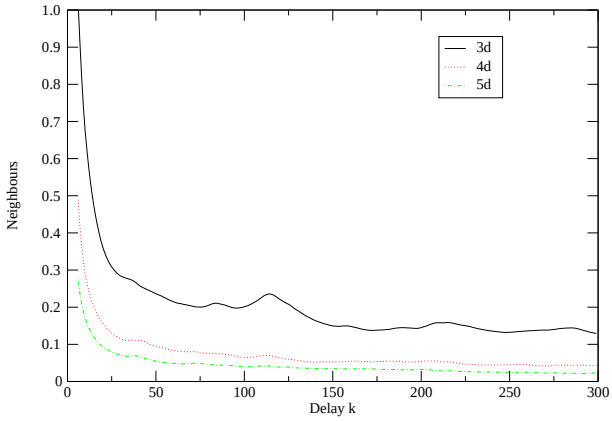

Figure 2: Number (in millions) of neighbouring pairs of points in the $\epsilon = 0.45$ dataset for different values of the delay k and different imbedding dimensions. False neighbours are the difference between consecutive curves.

not. This is, we ask whether $\mathcal{B}F(x, v, \phi)(t)$ can be considered a flow or not. Assuming boundedness of the reconstructed space, we consider the following indicators:

$$K_{max} = \sup_t \frac{d(\mathcal{B}F(x, v, \phi)(t + \Delta) - \mathcal{B}F(x', v', \phi')(t + \Delta))}{d(\mathcal{B}F(x, v, \phi)(t) - \mathcal{B}F(x', v', \phi')(t))} \tag{3}$$

$$K_{min} = \sup_t \frac{d(\mathcal{B}F(x, v, \phi)(t - \Delta) - \mathcal{B}F(x', v', \phi')(t - \Delta))}{d(\mathcal{B}F(x, v, \phi)(t) - \mathcal{B}F(x', v', \phi')(t))} \tag{4}$$

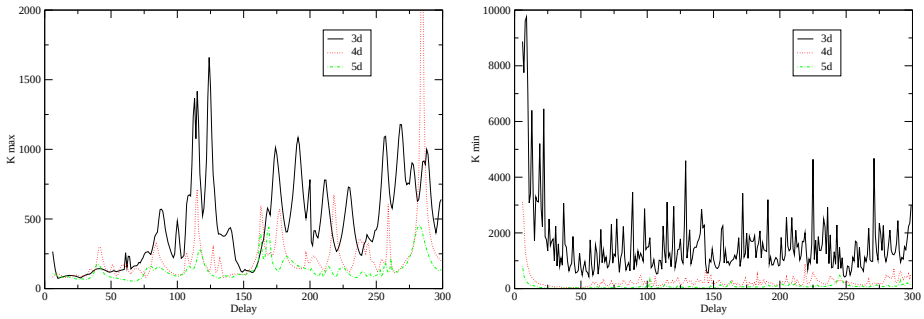

Figure 3: K_{max} and K_{min} tests for different values of the delay k and different imbedding dimensions. The test time was arbitrarily taken as $\Delta = 70$ ($\epsilon = 0.45$).

If $\mathcal{B}F$ is an imbedding, the flow in the reconstructed attractor is conjugated

to the flow in phase-space. In such a case, regarding Δ as a multiple of the sampling time, K_{max} represents an estimate (from below) to the Lipschitz constant of the flow on the imbedded manifold. Similarly K_{min} estimates the Lipschitz constant of the inverse (time-reversed) flow. If, on the contrary, $\mathcal{B}F$ is a projection, then pairs of points that lie relatively close to each other *after* projection, may have separated forward images after projection. Conversely, distant points may have closer images after projection, thus yielding larger values of K_{max} and K_{min} respectively. In short, if the K-values for a class of $\mathcal{B}F$-imbeddings are systematically larger than those for higher-dimensional alternatives, we can interpret this as a negative indicator: It is proper to suspect that $\mathcal{B}F$ is not an imbedding. We will illustrate a practical use of these estimators with the forced oscillator of eq.(2) in a coming subsection.

The test proposed above does not use the particular properties of forced oscillators. On the contrary, the next proposal is restricted to them. According to Lemma 1, as a result of the projection in forced oscillators, two points differing in their phase are assigned to the same projected point. Then, a $\mathcal{B}F$-imbedding can be put to test by considering the time-difference between close returns in the reconstructed data. This time-difference should be an integer multiple of the period in an imbedding, but it may present other values, possibly a broad collection of values, if the $\mathcal{B}F$-imbedding turns out to be a projection with additional (spurious) returns.

5.1 Examples of application I

First, we will present the results corresponding to the attractor of (2) for $\mu = 1.0434$, $\nu = -1$, $\omega = 0.399$ and $\epsilon = 0.45$. We check $\mathcal{B}F$-imbeddings of the form: $x_i, x_{i+5} - x_i, \ldots x_{i+km}$ following the proposal in [35]. In these units, the period of the forcing term is 300, $k = 6 \ldots 299$ and $m = 1 \ldots 3$ gives the dimension of the $\mathcal{B}F$-imbedding as $m + 2$. Higher-dimensional imbeddings were tested but are not presented here to keep the graphs as simple as possible. The data sets under study correspond to 1000 periods of the forcing term.

A neighbour detection for each $\mathcal{B}F$-imbedding is displayed in Figure 2. False neighbours can be estimated by the difference between consecutive curves. Observe that the number of neighbours diminishes monotonically with m for any delay, as expected. The number of neighbours roughly diminishes also for longer delays (large k). We could interpret this as a consequence of the divergence of nearby trajectories in chaotic flows, what makes the discrimination more efficient for longer delays.

Next we consider the test K_{max}, eq. (3). Results are displayed in Figure 3. The 3-dimensional imbedding appears to be reasonable, i.e. roughly equivalent to the procedures in higher dimensions, only in a region of delays below $k = 75$ and in a second region around $k = 150$.

These two tests are roughly compatible with the findings in [35]. We may argue that there are indeed two delay regions where the 3-d $\mathcal{B}F$-imbeddings seem to behave somewhat better than for all other delays. Note that in [35] and many other precedent and subsequent papers, only tests along the one in

Figure (2) were done.

On the other hand, when the test K_{min}, eq. (4), is considered (see Figure 3), we verify that 3-d $\mathcal{B}F$-imbeddings fail for all delay values while the 4-d alternatives appear to be acceptable, at least in a region around $k = 50$.

The strong dependence of the K_{min} value with the value k of the delay occurring in the 3d $\mathcal{B}F$-imbeddings, also contradicts a standard expectation regarding delay imbeddings, since the delay is not supposed to be a critical variable. On the contrary, the higher dimensional imbeddings do not contradict this expectation.

Hence, so far the tests already suggest that **none** of the 3-d $\mathcal{B}F$-imbeddings is a true imbedding since they fail the test K_{min}. In the light of this result we learn now that the slightly worse performance of the 3-d $\mathcal{B}F$-imbedding in the two initial tests was indeed decisive. To confirm this conclusion we study the time-intervals between close returns for one of the best candidates, with delay $k = 50$. We plot $-\log(d)$ against t, where d is the distance measured in the $\mathcal{B}F$-imbedding and t the time between d-close returns (in sampling-time units), comparing the results for 3d and 4d $\mathcal{B}F$-imbeddings. Larger values of $-\log(d)$ correspond to closer returns. We observe in Figure 4 that there exist recurrences in the 3d $\mathcal{B}F$-imbedding that are removed in 4d. These returns occur at intermediate periods and suggest spurious close returns arising as a consequence of the projection. Note that the return times in the 4d alternative are well-tuned with the period of the forcing.

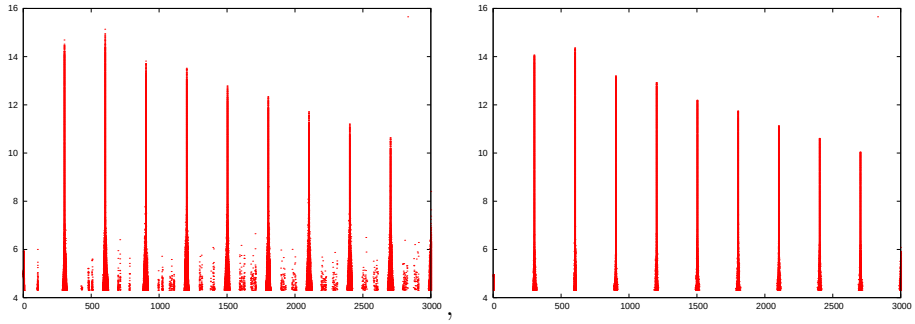

Figure 4: Detection of the natural period. Left: 3d procedure. Note the spurious dots between peaks and the relatively thick periodic peaks. Right: 4d procedure. The spurious dots have dissappeared and the peaks are sharper at the base. Larger values on the y-axis correspond to closer returns ($\epsilon = 0.45$).

5.2 Examples of application II

We consider here a slightly different situation for the same eq. (2), in this case setting $\epsilon = 0.452$. Figures (5)–(7) reproduce the computations of the previous subsection for the present case.

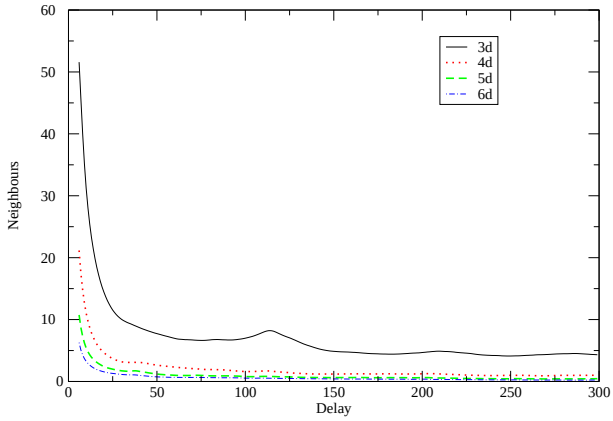

Figure 5: Number (in millions) of neighbouring pairs of points in the $\epsilon = 0.452$ dataset for different values of the delay k and different imbedding dimensions. False neighbours are the difference between consecutive curves.

The false neighbours test of Figure 5 again displays a systematically better performance when increasing the imbedding dimension. The optimal delay value for 3d seems to lie near $k = 250$, but the number of detected neighbours is about a factor of 10 larger than for 4d procedures. The scale of the graph does not allow to draw conclusions about how "good" the 4d procedure could be when

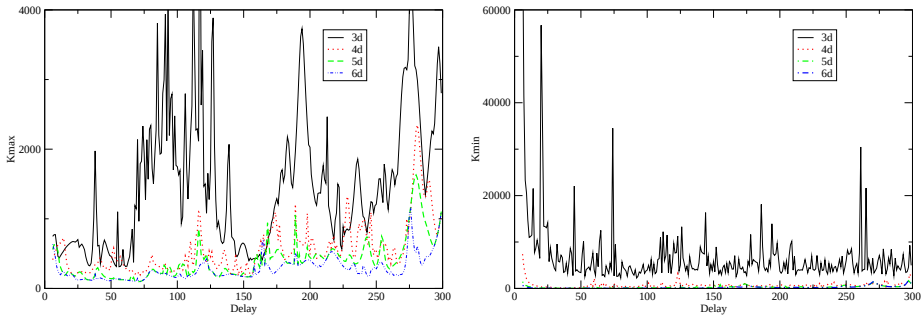

Figure 6: K_{max} and K_{min} tests for different values of the delay k and different imbedding dimensions. The test time was arbitrarily taken as $\Delta = 70$ ($\epsilon = 0.452$).

The test K_{max} (Figure 6) displays now an unacceptable performance both in dimensions 3 and 4, while the unsuccessful performance of dimension 3 in K_{min} (Figure 6) renders the scale insufficient to read any differences in higher dimensions.

Finally, the detection of the natural period (Figure 7) displays returns (although not very *close*) for essentially all investigated time-intervals in dimension 3.

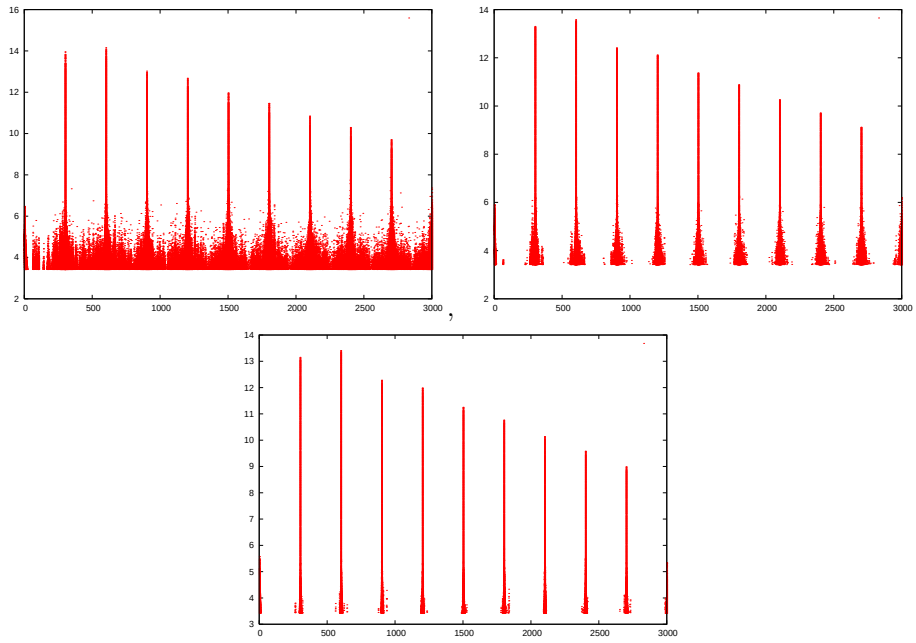

Figure 7: Detection of the natural period. Upper left: 3d procedure. Note the abundant spurious dots between peaks and the relatively thick periodic peaks. Upper right: 4d procedure. Part of the spurious dots persist although the peaks are getting sharper at the base. Second row: 5d procedure. The peaks are now much sharper. Larger values on the y-axis correspond to closer returns ($\epsilon = 0.452$).

The overall picture given by these tests is that a relatively small change in the system parameters produced a dramatic worsening of the performance of different $\mathcal{B}F$-imbedding procedures. Not only are the 3d candidates in this case clearly insatisfactory, but even the 4d computations may also be insufficient.

6 Imbedding techniques for Periodically Forced Oscillators

The results in Figures 4 and 7 indicate a correct way to proceed in order to generate dynamical data from a recorded variable of a periodically forced oscillator. It is an immediate fact arising from eq. (1) that recording the two variables (x_i, ϕ_i) of a periodically forced oscillator, then we can reconstruct the original phase-space data, for sufficiently small sampling intervals. First we

numerically compute the time-derivative of the x-array and from each pair of recorded variables generate a point of phase-space, namely (x_i, v_i, ϕ_i), to within the accuracy of the recording and numerical procedures.

If, as it has been frequently the case, ϕ is lacking from the experimental records, still the numerical evidence from the Figures strongly supports the assumption that there exists in the data a natural period where the quality and extent of the close returns is several orders of magnitude better than for any other return-time (one unit of the vertical axis corresponds to a factor of e). There is a clear difference (detectable already by inspection) between the height of the regular peaks in both figures and the typical height of the irregular part of the graph. Note also that the quality of the sharp peaks deteriorates for increasing time, being this compatible with the fact that the sampled data arises from orbits lying in the vicinity of unstable period-1 or period-2 orbits, hence longer return times accumulate larger errors.

Periodically forced oscillators cannot have other periodic orbits than those given by the returns on the Poincaré section. It is hence a given assumption that the natural period of the data corresponds to a multiple of the forcing period. In this way we can associate to each data point x_i a phase-value $\psi_i = 2\pi/T$, where T is the natural period given by inspection of Figures (4) and (7). In the present case we have $T = 300$.

The data in this manuscript was numerically integrated using a computer program, hence the sharp peaks with periodicity $T = 300$ in Figures 4 and 7. For the model problems analyzed in this manuscript, the reconstructed data sets $(x_i, \dot{x}_i, \psi_i)$, $i = 1, \cdots, N$ coincide up to numerical accuracy with the outcome of the numerical integration of eq. (2). In a typical experimental setup, the forcing period need not be an integer multiple of the sampling time, and some subsequent estimation procedure for the forcing period may be required.

7 The Issue of Topologically Inequivalent Imbeddings

In the light of these findings, the results in [35] deserve reevaluation. Is it possible that two bona-fide imbedding procedures yield topologically inequivalent results, e.g., different braid-types for the same orbit? Let us try to understand how and why this could be possible.

One source of inequivalences for periodically forced oscillators may lie in the fact that there exist inequivalent control sections. Indeed, the oscillator in eq.(2) has the trivial periodic orbit $(0, 0, \phi)$. A control section $\phi = \phi_0$ represents this orbit as a fixed point. On the other hand, a control section $\dot{x} = v_0$ cannot detect this orbit (not even for $v_0 = 0$, when it would entirely lie on the control section), but it will still detect all periodic orbits linked with the trivial one. For the choice $v_0 = 0$, the period of the orbits in this control section will increase by a factor given by their linking number with the trivial orbit.

Another source of inequivalences may be that it may not be possible to

extend a bona-fide procedure to the whole of phase space, although it seems to work for a limited data set. As a general rule, when the available data leaves large portions of phase-space unsampled or poorly sampled, different procedures may handle the data in different and inequivalent ways. Essentially, two different imbedding procedures may yield two different ways of imbedding a closed curve in a three dimensional space. However, topological assertions about the imbedded orbits carry assumptions about the complement of the orbit in phase space. If the data has insufficient sampling in this complement, there is no way to support these assumptions.

If the data collection is improved in the sense of extending the well-sampled region of phase space (for example, incorporating trajectories in the basin of attraction of the invariant attractor) to the point that all periodic points can be detected, immersed in a sea of data points sampling a topological disk in the Poincaré section, then, having reached this point we also reach the certainty that at least one of the bona-fide procedures yielding inequivalent topological properties actually was not an imbedding. Hence, in order to interpret experimental data, it is advisable to render explicit the additional hypotheses not supported in the actual data and to keep them to a minimum.

In the particular case in which topological inequivalent "imbeddings" have been reported [35] the word imbedding refers to the imbedding of a periodic orbit in R^3 (or of S^1 in R^3). The "imbeddings" do not represent a disk in the Poincaré section but rather three disjoint disks. By the above reasoning, they cannot both be extended to a whole disk in the Poincaré section, a fact already recognized in [35], where one goal was to address naive and "black-box" use of topological implications. Furthermore, none of the proposed imbedding procedures passes the more demanding tests introduced in this work, so they are not satisfactory candidates in the first place.

However, two procedures that properly identify the control section $\phi = \phi_0$ and that can be extended to all of phase space, will render the same braid types for all orbits, this is a consequence of the nature of the space $R^2 \times S^1$ inspiring the definition and elaboration of the concept of braid type [40, 46].

8 Conclusions

We have explored some possible imbedding methods for attractors in periodically forced oscillators (1), particularly looking for 3-d reconstructions allowing for topological analysis of the attractor. In this exploration we have shown that reconstructions of the form $(x, \dot{x}, x_3)_i$ are projections from phase-space (and not imbeddings) for broad choices of x_3 including delay coordinates. We have further demonstrated that such projections do not produce a flow in the projected space as a projection of the flow in phase space.

While x alone as information source appears to be insufficient to describe periodically forced oscillators with 3-d imbeddings, the pair (x, ϕ) does provide a complete description of the system. In optimal sampling situations, the phase ϕ can be estimated from the time-series of x. By considering the characteristic

times of the close returns it is possible to detect the clock. Thus, effectively sampling the phase ϕ as the measured time.

This newly gained perspective suggests how *false neighbours* tests can be complemented with new tests. In the examples we explored, the new tests allowed to discard proposed imbeddings that previously could pass the controls based on false neighbours only.

Indeed, a drawback of the false neighbours test is that if the data contains periodic orbits, then the test will persist detecting neighbours across many dimensions. There is therefore some arbitrariness in deciding when to stop the procedure and declaring a given imbedding dimension as optimal. The new checks K_{max} and K_{min} on the contrary, consider if a smooth flow is compatible with the proposed imbeddeding of the data. Here, the existence of periodic orbits will not influence the estimates. For the special case of periodically forced oscillators, the return times test exploits the periodicity of the forcing to accept or reject proposed imbeddings.

We summarise the conclusions as an itemlist:

- Dynamical reconstructions of the form $(x, \dot{x}, x_3)$ are projections from phase-space and not imbeddings.
- The coordinate pair (x, ϕ), on the other hand, does provide a complete description of the system (from which a good imbedding can be extracted). In optimal sampling situations, the phase ϕ can be estimated from the time-series of x.
- The method of *false neighbours*, although a good indicator, is not sensitive enough to discriminate between imbeddings and not-imbeddings.

9 Acknowledgments

HGS acknowledges a grant from the University of Buenos Aires. MN acknowledges a travel grant from Vetenskapsrådet to participate in the 2007 SIAM Conference on Applications of Dynamical Systems. HGS and MN thank especially Kevin Mitchell and Pieter Collins, the organizers of the mini-symposium Topological Methods for Low Dimensional Chaotic Systems, for their kind invitation.

References

[1] G Duffing. *Erzwungene Schwingungen bei Veränderlicher Eigenfrequenz und ihre Technische Bedeutung.* Vieweg, Braunschweig, 1918.

[2] van der Pol. A theory of the amplitude of free and forced triode vibrations. *Radio Review*, 1:701–762, 1920.

[3] J. Guckenheimer and P. J. Holmes. *Nonlinear Oscillators, Dynamical Systems and Bifurcations of Vector Fields.* Springer, New York, 1986. 1st printing 1983.

[4] J Sacher, D Baums, P Pauknin, Wolfgang Elsässer, and E O Göbel. Intensity instabilities of semiconductor lasers under current modulation. *Phys. Rev.*, 45 A:1893, 1992.

[5] A N Šarkovskii. Coexistence of cycles of a continuous map of a line into itself. *Ukr. Mat. Z.*, 16:61, 1964.

[6] N Metropolis, M L Stein, and P R Stein. On finite limit sets for transformations on the unit interval. *J. Combinatorial Theory*, 15A:25, 1973.

[7] J. Franks. Knots, links and symbolic dynamics. *Annals of Mathematics*, 113:529–552, 1981.

[8] J. Franks and R. F. Williams. Entropy and knots. *Trans. American Mathematical Society*, 291:241–253, 1985.

[9] W P Thurston. On the geometry and dynamics of diffeomorphisms of surfaces. *Bull. Am. Math. Soc.*, 19:417, 1988.

[10] T Hall. Unremovable periodic orbits of homeomorphisms. *Math. Proc. Camb. Phil. Soc.*, 110:523–531, 1991.

[11] M Bestvina and M Handel. Train tracks and automorphisms of free groups. *Annals of Mathematics*, 135:1–51, 1992.

[12] John Franks and Michal Misiurewicz. Cycles for disk homeomorphisms and thick trees. *Contemporary Mathematics*, 152:69–139, 1993.

[13] Toby Hall. Fat one-dimensional representatives of pseudo-anosov isotopy classes with minimal periodic orbit structure. *Nonlinearity*, 7:367–384, 1994.

[14] H G Solari and M A Natiello. Minimal periodic orbit structure of 2-dimensional diffeomorphisms. *Journal of Nonlinear Science*, 15(3):183–222, 2005.

[15] Natiello M A and Solari H G. *The User's Approach to Topological Methods in 3d Dynamical Systems.* World Scientific, New York, 2007.

[16] H G Solari and R Gilmore. Relative rotation rates for driven dynamical systems. *Phys. Rev.*, 37A:3096, 1988.

[17] H G Solari and R Gilmore. Organization of periodic orbits in the driven duffing oscillator. *Phys. Rev.*, 38A:1566–1572, 1988.

[18] G. B. Mindlin, Xin-Jun Hou, R. Gilmore, H. G. Solari, and N.B. Tufillaro. Classification of strange attractors by integers. *Physical Review Letters*, 64:20, 14 May 1990.

[19] G. B. Mindlin, H. G. Solari, M. Natiello, R. Gilmore, and Xin-Jun Hou. Topological analysis of chaotic time series data from the belusov-zhabotinskii reaction. *Journal of Nonlinear Sciences*, 1:147–173, 22 April 1991.

[20] F Takens. Detecting strange attractors in turbulence. In D A Rand and L-S Young, editors, *Lecture Notes Math.*, volume 898, page 366. Springer, Berlin, 1981.

[21] N Packard, J Crutchfield, and R Shaw. Geometry from a time series. *Phys. Rev. Lett.*, 45:712, 1980.

[22] Stark J. Delay embeddings for forced systems. i. deterministic forcing. *J Nonlinear Science*, 9:255–332, 1999.

[23] H Whitney. The self-intersections of a smooth n-manifold in 2n-space. *Ann. Math.*, 45:220–246, 1944.

[24] H Whitney. Differentiable manifolds. *Ann. Math.*, 37:654, 1936.

[25] H D I Abarbanel, R Brown, J J Sidorowich, and L Sh Tsimring. The analysis of observed chaotic data in physical systems. *Rev. Mod. Phys.*, 65:1331, 1993.

[26] Yung-Chia Hsiao and Pi-Cheng Tung. Controlling chaos for nonautonomous systems by detecting unstable periodic orbits. *Chaos, Solitons & Fractals*, 13:1043–1051, 2002.

[27] Abraham C.-L. Chian, Felix A. Borotto, Erico L. Rempel, and Colin Rogers. Attractor merging crisis in chaotic business cycles. *Chaos, Solitons & Fractals*, 24:869–875, 2005.

[28] Abraham C.-L. Chian, Erico L. Rempel, and Colin Rogers. Complex economic dynamics: Chaotic saddle, crisis and intermittency. *Chaos, Solitons & Fractals*, 29:1194–1218, 2006.

[29] Chunbiao Gan and Shimin He. Surrogate test for noise-contaminated dynamics in the duffing oscillator. *Chaos, Solitons & Fractals*, 38:1517–1522, 2008.

[30] S.G. Stavrinides, N.C. Deliolanis, Th. Laopoulos, I.M. Kyprianidis, A.N. Miliou, and A.N. Anagnostopoulos. The intermittent behavior of a second-order non-linear non-autonomous oscillator. *Chaos, Solitons & Fractals*, 36:1191–1199, 2008.

[31] Rafal Rusinek and Jerzy Warminski. Attractor reconstruction of self-excited mechanical systems. *Chaos, Solitons & Fractals*, 2007. In press. Available on-line.

[32] F A McRobie. Bifurcation precedences in the braids of periodic orbits of spiral 3-shoes in driven oscillators. *Proceedings R. Soc. Lond. A: Mathematical and Physical Series*, 438:545–569, 1992.

[33] M Huerta, D Krmpotic, G B Mindlin, H Mancini, D Maza, and C Pérez-García. Pattern dynamics in a benard-marangoni convection experiment. *Physica D*, 96:200–208, 1996.

[34] D Krmpotic and G B Mindlin. Truncating expansions in bi-orthogonal bases: What is preserved? *Physics Letters A*, 236:301–306, 1997.

[35] G.B. Mindlin and H.G. Solari. Topologically inequivalent embeddings. *Phys. Rev.*, E52:1497, 1995.

[36] Tsvetelin D. Tsankov, Arunasri Nishtala, and Robert Gilmore. Embeddings of a strange attractor into r^3. *Physical Review E*, 69:056215–1:8, 2005.

[37] N Romanazzi, M Lefranc, and R Gilmore1. Embeddings of low-dimensional strange attractors: Topological invariants and degrees of freedom. *Physical Review*, E75:066214, 2007.

[38] G Vaschenko, M Giudici, J J Rocca, C S Menoni, J R Tredicce, , and S. Balle. Temporal dynamics of semiconductor lasers with optical feedback. *Phys. Rev. Lett.*, 81:5536–5539, 1998.

[39] G Huyet, S Balle, M Giudici, C Green, G Giacomelli, and J R Tredicce. Low frequency fluctuations and multi-mode operation of a semiconductor laser with optical feedback. *Opt. Commun.*, 149:341–347, 1998.

[40] T Hall. The creation of horseshoes. *Nonlinearity*, 7:861, 1994.

[41] T Ondarchu, G B Mindlin, H L Mancini, and C Pérez García. Dynamical patterns in benárd-marangoni convection in a square container. *Physical Review Letters*, 70:3892–3895, 1993.

[42] J Guckenheimer and P Holmes. Structurally stable heteroclinic cycles. *Math. Proc. Cambridge Phil. Soc.*, 103:189, 1988.

[43] C Letellier and R Gilmore. Covering dynamical systems: Twofold covers. *Physical Review E*, 63:016206, 2000.

[44] C Letellier, L A Aguirre, and J Maquet. Relation between observability and differential embeddings for nonlinear dynamics. *Physical Review*, E71:066213, 2005.

[45] D. P. Lathrop and E. J. Kostelich. Characterization of an experimental strange attractor by periodic orbits. *Physical Reviews A*, 40:4028–4031, 1989.

[46] M A Natiello and H G Solari. Remarks on braid theory and the characterisation of periodic orbits. *J. Knot Theory Ramifications*, 3:511, 1994.

[47] M W Hirsch. *Differential Topology*. Springer, New York, 1976.

Appendix I: Basic summary on imbeddings

An imbedding[3] consists of two parts. First a map $f : M \to N$ (of an m-dimensional manifold M to a manifold N) that is homeomorphic onto the image, i.e., f is injective and continuous, and the inverse map defined from $f(N)$ to M is also continuous. Further, the induced map between tangent spaces at each point of M is injective (this is called an *immersion*), i.e., m independent directions at T_x are mapped onto m independent directions at $T_{f(x)}$.

The imbedding of abstract manifolds in R^n is treated in the theorems of Whitney [24]. The simplest theorem states that any compact Hausdorff[4] manifold of class C^r ($r \geq 1$) can be imbedded in R^n, for n large enough. The idea behind this statement is that since a compact manifold is defined by a finite set of local charts[5], we may build an imbedding satisfying the definitions more or less by putting these charts "beside" each other so that their images land in different dimensions on a huge-dimensional space [47]. The famous imbedding theorem of Whitney states that compact, Hausdorff, C^r ($r > 1$ this time) manifolds can be imbedded in R^{2m+1} [47]. Further refinements have been produced, e.g., a similar result holds for non-compact manifolds, it holds already with $r = 1$, already dimension $2m$ is enough to imbed any manifold (but for special classes of manifolds the minimal imbedding dimension is even lower), etc.

Part of the intuition behind Whitney's proof was based on approximations: Given *any* C^r map $g : M \to R^{2m+1}$, there is an imbedding f arbitrarily close to it (i.e., for any positive ϵ an imbedding f can be found such that for all $x \in M$, $|f(x) - g(x)| < \epsilon$ [47]).

Takens [20] profitted of the approximation approach and realized that given a smooth real-valued outcome function of a dynamical system with a smooth vector field X (and associated flow $\Phi_t(x)$), then it is a generic[6] property that the construction $(y(x), y(\Phi_\delta(x)), \cdots, y(\Phi_{2m\delta}(x)))$ is an imbedding of the original manifold (where $\Phi_t(x)$ lives) on R^{2m+1}.

[3]There are many spellings of this word circulating in the literature. We adopt the spelling used by Whitney [24] in his fundamental work.

[4]i.e., *separated*. Most "natural" manifolds in applications are Hausdorff.

[5]C^r-smooth maps from finite open connected regions to R^m.

[6]In this context, *generic* means that the set of functions y and vector fields X yielding imbeddings is an open and dense subset of the set of all smooth functions and smooth vector fields.